AUT Journal of Electrical Engineering

AUT J. Elec. Eng., 58(3) (2026) 553-570
DOI: 10.22060/eej.2026.24324.5683

Intelligent Photovoltaic Conversion System with Cascaded Fuzzy MPPT for Efficient DC Power Transfer

Golla Satyanarayana[1]*, Tappeta Amai Kiran[2], Rushan Kumar[1], Kodi Yohan1, Mokim Ansari[1]

[1] Department of Electronic Engineering, Godavari Institute of Engineering Science and Technology (A), Rajahmundry.
[2] Department of Electronic Engineering, Godavari Global University, Rajahmundry.

ABSTRACT: In most areas and power systems, Photovoltaic (PV) energy is rapidly becoming a significant component of the energy balance because of its rapid annual growth rate. Therefore, this research presents the PV-fed improved SEPIC-Zeta converter with a cascaded fuzzy algorithm-based Maximum Power Point Tracking (MPPT) for efficient DC power transfer. At the beginning, the improved SEPIC-Zeta (ISZ) converter is exploited to enhance the PV system's voltage. Then, the Cascaded Fuzzy MPPT algorithm is introduced for tracking the upmost power from the PV system. Also, the high-frequency inverter transmutes the DC to AC power, and isolation is provided by the isolation transformer to ensure safety and mitigate harmonic distortion on the source and load side. Additionally, the interleaved synchronous rectifier is exploited for converting the AC into a DC supply. The implemented research is validated in the MATLAB tool, which demonstrates that the proposed work has a converter efficacy of 95.12 %, which handles fluctuations and disturbances more effectively, enhancing the reliability of the overall system.

Review History:
Received: Jun. 27, 2025
Revised: Feb. 24, 2026
Accepted: Apr. 21, 2026
Available Online: Jul. 01, 2026

Keywords:
PV System
ISZ Converter
Cascaded Fuzzy MPPT Algorithm
High Frequency Inverter
Isolation Transformer

1- Introduction

The incorporation of non-renewable and renewable electrical power plants for simultaneous use in national transmission systems is mandated by the profusion of Renewable Energy Resources (RESs) and the low cost of power generation [1]. Globally, power systems that rely on fossil fuels are giving way to those that rely on RES [2-4]. Conventional energy sources are not the best option to meet this energy need because of their limited supply, unstable pricing, and issues with greenhouse gas emissions [5–6]. One of the most accessible energy sources is solar energy, which is cleanly transformed into electric power via PV systems [7-9]. Although solar energy is abundant, its harvest is constrained by its efficiency. Variations in solar radiation, the impacts of shadowing, and the growth in solar cell temperature are some of the factors that negatively impact the performance of PV systems [10–11]. It causes variations in the fundamental properties of solar PV systems, which in turn cause variations in voltage [12–13]. Therefore, to generate high voltage on the output side, a DC/DC converter is needed [14]. A Boost converter is developed in [15] with low inductor current and non-pulsating input current. However, the efficacy of a boost converter decreases because of switching and conduction losses. A SEPIC converter, which has a non-inverting configuration, is presented in [16]. Nevertheless, at higher duty ratios, this converter is no longer capable of producing considerable voltage gain. In [17], a Cuk converter is developed that has the lowest switching losses, the lowest voltage ripple, and high efficiency. Nevertheless, the switch in the Cuk converter experiences high current stress due to the dynamic operation, which affects reliability. A Zeta converter with a non-inverted output voltage is represented in [18]. However, the input current is irregular, making it unsuitable for certain applications that need a constant input current. The Modified SEPIC converter has better transient response and lower output voltage ripple, as presented in [19]. However, it has a complex structure, and the performance is sensitive to its component values. Therefore, this work proposes an ISZ converter for improving the PV system's voltage. An MPPT is necessary to enhance the power conversion efficacy of a PV system due to its nonlinear power-voltage (P-V) characteristics [20]. Also, it is necessary in this converter in order to completely utilize the PV panel's capacity [21]. Numerous MPPT strategies have been documented to increase the PV system's power conversion MPPT efficacy. The P&O MPPT is developed in [22], withstands abrupt deviations in temperature and irradiance because it successfully and efficiently adheres to the MPP. Conversely, the P&O has to choose between steady-state oscillations and dynamic responsiveness (speed).

A hill-climbing MPPT algorithm with a minimal cost and a straightforward control mechanism is presented in [23].

*Corresponding author's email: satyanarayanag479@yahoo.com

Table 1. Analysis with research literature.

REFERENCE	MERITS	DRAWBACKS
[27]	• The reliance on the grid is reduced. • It enhances the efficacy and decrease the operational expense. • It enable the system to efficiently regulate and adapt to real world nonlinearities.	• It has maximum investment expense for EVCS. • It has slower convergence speeds and more difficult due to the advanced control approach. • The efficacy of stochastic model depends on comprehensive and accurate dataset to efficiently train the system.
[28]	• Reduces charging time and allows effective charging. • It efficiently tracks the upmost power and better voltage gain. • It attains enhanced reliability with better MPPT action.	• It has difficulties in implementation and maintenance. • It incorporates significant design and control complexity. • It needs careful management and an extended development time.
[29]	• The overall efficacy is enhanced. • It quickly converges to the MPP while dynamic charging conditions need quick power adjustments. • High resilience to parameter changes, making it reliable for real-world EV charging.	• The implementation and design are difficult. • First-order sliding mode induces high-frequency switching. • It necessitates battery storage or grid backup for continuous EV supply.
Proposed	• It enhances the PV system's low voltage. • It offers isolation between the PV and DC bus for protecting sensitive elements.	• Assessing the system performance in a large-scale microgrid environment with a hybrid energy storage solution to enhance grid stability needs to be considered.

It will run at the local MPP, which results in low system efficacy; it is not appropriate for partially shaded situations. In [24], an Incremental Conductance-based MPPT, which continuously alters the operating point, guarantees that the PV system functions at its highest efficiency. Nevertheless, the continuous calculation of incremental conductance increases the computational load on the system. In [25], an Artificial Bee Colony-based MPPT is developed, which is relatively simple to implement. Nevertheless, there is a danger of early convergence to suboptimal solutions if the diversity of the search agents is not maintained. A Fuzzy logic MPPT algorithm with the advantages of nonlinearities, faster response times, and handling imprecise inputs is developed in [26]. However, it causes inefficiency by producing strong oscillations around the MPPT. Table 1 signifies the analysis of existing research literature.

As a result, this work proposes a cascaded fuzzy MPPT algorithm, which tracks the highest power from the PV system. The main objectives are,

- To improve the PV system's low voltage, an ISZ converter is exploited.
- For tracking the maximum power from the PV panel, a cascaded fuzzy MPPT algorithm is exploited.
- For an effective power conversion process, the HFI and isolation transformer are employed, which provides isolation between PV and DC bus for protecting sensitive elements.
-

2- Proposed Methodology

This research proposes a PV-based ISZ converter with a cascaded fuzzy MPPT algorithm for low-voltage applications. Fig. 1. Represents the developed work's block diagram for efficient power transfer.

Initially, the PV system's voltage is fed to an ISZ converter that improves its voltage. Then, the output current PV system and voltage is given to the cascaded fuzzy MPPT that tracks the maximum power from PV system. Subsequently, the PWM generator generates the pulses for the converter's better switching function. The ISZ converter's output is delivered to the HFI, which alters the DC to AC voltage, which is given

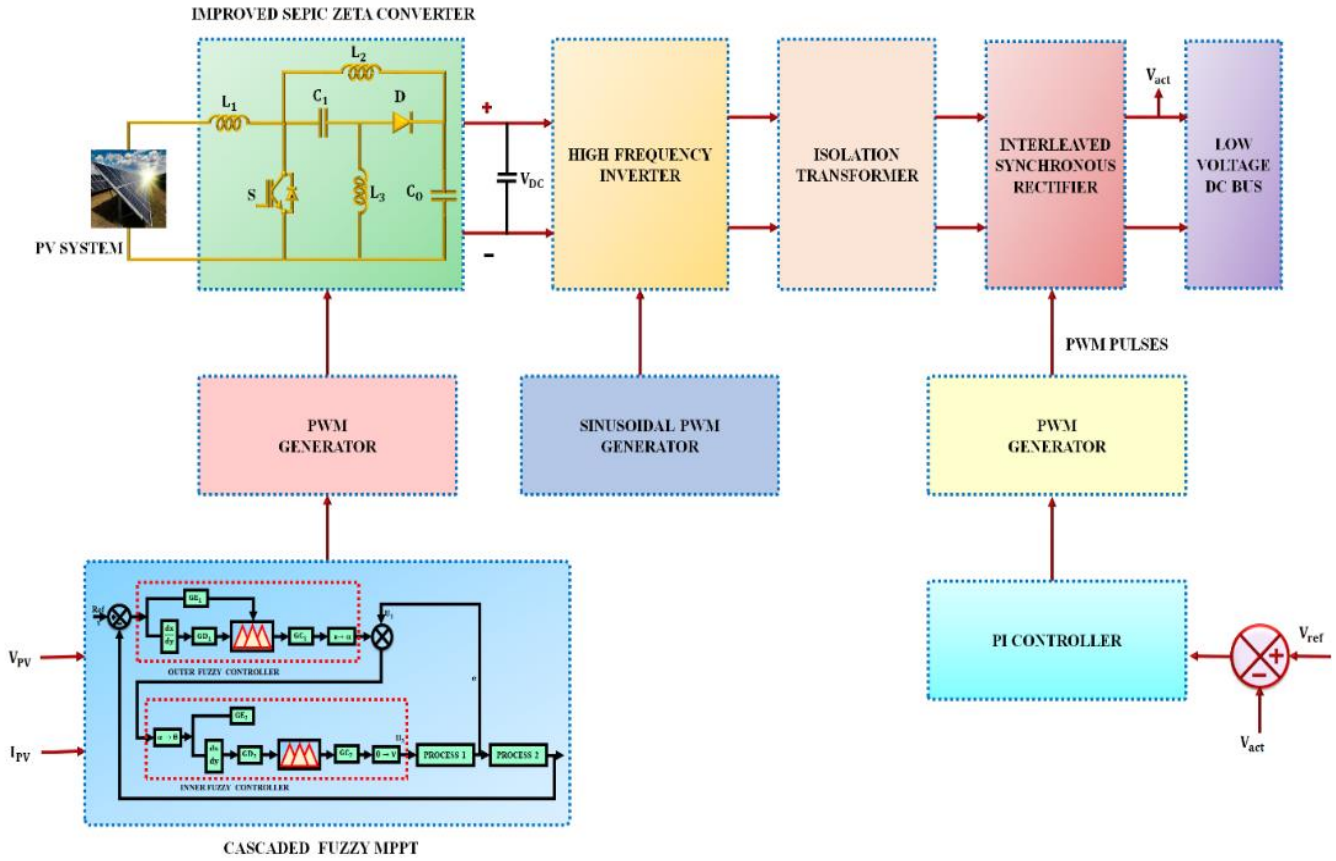

Fig. 1. Developed work's Block diagram.

to the isolation transformer. The high-frequency AC voltage is passed through an isolation transformer to ensure electrical isolation and to step down or up the voltage as required. The output from the transformer is rectified back to DC using an interleaved synchronous rectifier, which improves efficacy by decreasing switching losses. The rectified output is delivered to a low-voltage DC bus, which is exploited to power loads. Also, the PI controller manages the rectifier, and pulses are created by a PWM generator for the switching function of the inverter, ensuring the high-efficiency power conversion appropriate for renewable energy applications.

2- 1- PV System

The most important part of a PV system is the solar cell, which uses the PV effect to produce DC voltage when exposed to sunlight. In this case, the series resistance is R_S, The current on the output side is indicated by I , , The PV voltage is V , The shunt resistance is indicated by R_p and the diode current is I_D . The PV cell's circuit is presented in Fig. 2. The current equation of the PV panel is,

$$I = I_{PV} - I_O\left[e^{\frac{(v+R_S I)}{V_k \alpha}-1}\right] - \frac{V + I R_S}{R_p} \qquad (1)$$

Equation (1) offers factors that impact the functioning of a PV cell. Where high thermal voltage is represented by α , the diode's ideality constant is specified by V_k The saturation current of the PV system is indicated by I_O , The PV system produces a low voltage, which is passed into the ISZ converter.

2- 2- Improved SEPIC-Zeta Converter

The ISZ converter comprises both the SEPIC and Zeta converter, as revealed in Fig. 3. It consists of inductors L_3, L_1 and L_2, diode D, switch S, capacitors C_1 and C_O and output resistor R_O . It is operated in two stages:

Stage 1

In this stage, S is in conducting mode, D is reverse biased and L_1, L_2 and L_3 are charged, as represented in Fig. 4. The voltage on C_1 is discharged, which is identical to the input voltage V_{in} . Also, V_{in} is equivalent to the voltage across the inductors V_{L1} and V_{L3}. The current passing via S is the addition of current in inductors i_{L1} and i_{L2}. C_3 is charged and C_o is discharged.

Stage 2

Here, S is a non-conducting mode, L_1, L_2 and L_3 are discharged and D It is forward-biased in stage 2. Here, the input capacitor C_1 and output capacitor C_o are charged. Stage 2 of the converter is displayed in Fig. 5.

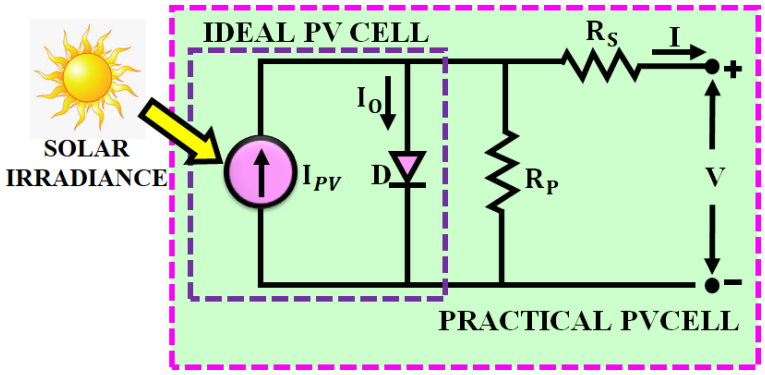

Fig. 2. Circuit of PV system.

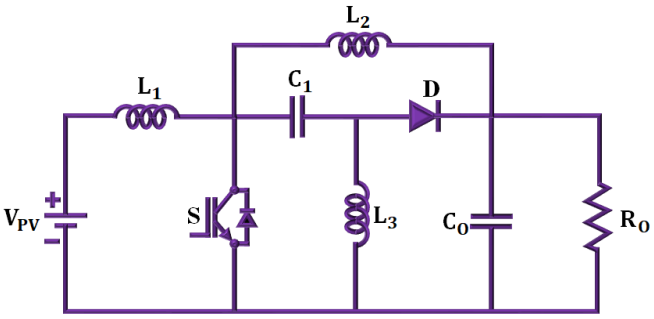

Fig. 3. ISZ converter.

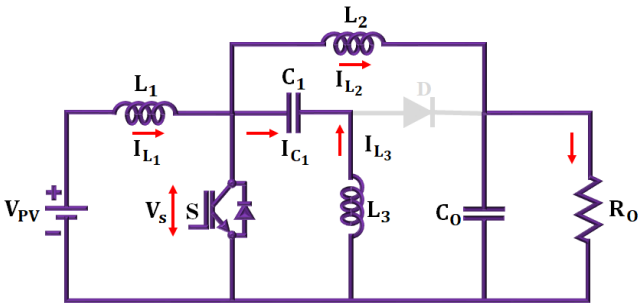

Fig. 4. Stage 1 of the ISZ converter.

In mode 1,

$$V_{L1} = V_{PV} \tag{2}$$

$$V_{L3} + V_{C1} = 0 \tag{3}$$

$$V_{PV} - V_{L1} - V_{L2} - V_{Co} = 0 \tag{4}$$

$$V_o = V_{Co} \tag{5}$$

In mode 2,

$$V_{PV} - V_{L1} - V_{C1} - V_{L3} = 0 \tag{6}$$

$$V_{Co} = V_{L3} \tag{7}$$

Utilizing equation (7) in (6)

$$V_{PV} - V_{L1} - V_{C1} - V_{Co} = 0 \tag{8}$$

By applying volt second balance principle,

$$V_{PV} D + (V_{PV} - V_o)(1 - D) = 0 \tag{9}$$

$$D(1 + V_{PV}) - V_o - V_{PV} D + D V_o = 0 \tag{10}$$

$$V_{PV}(1 - D) - V_o = 0 \tag{11}$$

$$V_o(1 - D) = V_{PV} \tag{12}$$

Where the voltage across L_3, L_2 and L_1 are V_{L3}, V_{L2} and V_{L1} voltage across C_3, C_1 and C_2 are V_{C3}, V_{C1} and V_{C2}, and the voltage on the output side is V_o. The voltage gain of

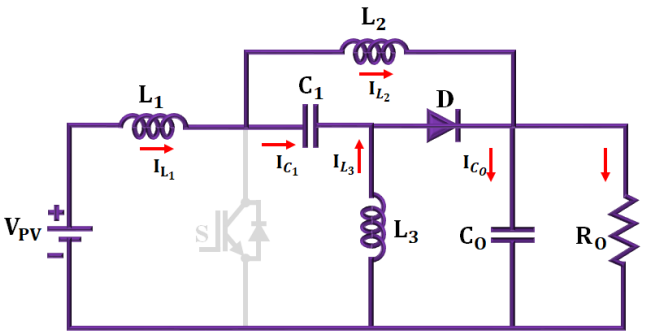

Fig. 5. Stage 1 of the ISZ converter.

the ISZ converter is,

$$M = \frac{V_o}{V_{PV}} = \frac{1}{1-D} \tag{13}$$

Fig. 6 illuminates the functional waveform of ISZ converter. For tracking the highest power from PV system, a cascaded fuzzy MPPT algorithm is employed.

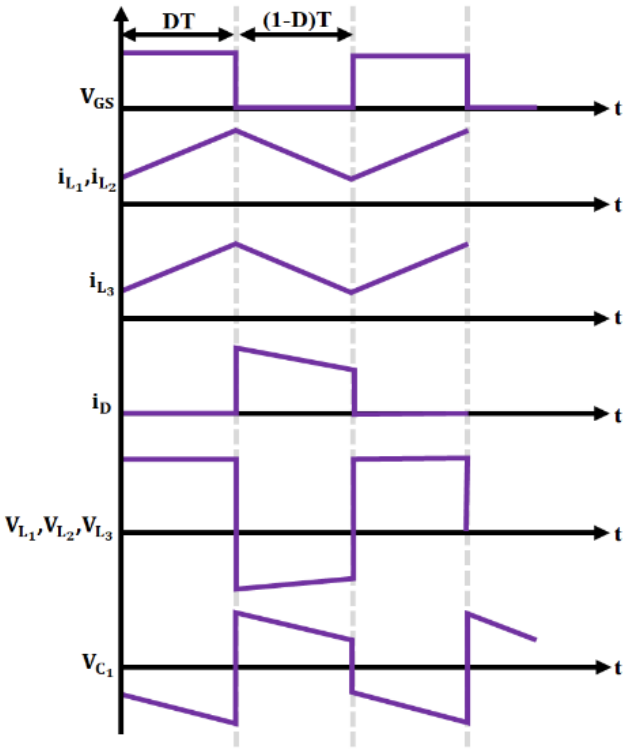

Fig. 6. Waveform of ISZ converter.

2- 3- Cascaded Fuzzy MPPT

An outer and inner controller are combined to develop two cascaded fuzzy controllers in a cascaded fuzzy MPPT technique. As indicated in Fig. 8, fuzzy controllers' inherent nonlinearity and ability to formalize control information make a creative and successful substitute for conventional control techniques. A fuzzy controller at an outer loop is produced by combining the following ideas:

$$R^k : E_i \ \ is \ \ A_1^k \ and \ \Delta E_i \ \ is \ \ A_2^k \ \ then \ U_i = B_k \tag{14}$$

In this case, $\mathrm{R^k - kth}$ rule $\left(\mathrm{k}\,1/4,1,2,\mathrm{y},\mathrm{m}\right)$, ΔE_i represents a change of error, E_i denotes error, A_1^k and A_2^k are fuzzy sets of linguistic values, U_i defines output, and B_k indicates a numeric control value.

$$Inner\ loop:\ min\left\{\mu_{A1k}(E), \mu_{A2k}(\Delta E)\right\} = w_{1k} \tag{15}$$

$$Outer\ loop:\ min\left\{\mu_{A1k}(E), \mu_{A2k}(\Delta E)\right\} = w_{2k} \tag{16}$$

$$-U_1^* = \frac{\sum_{k=1}^{m} w_{1k} B^k}{\sum_{k=1}^{m} w_{1k}} \tag{17}$$

$$U_2^* = \frac{\sum_{k=1}^{m} w_{2k} B^k}{\sum_{k=1}^{m} w_{2k}} \tag{18}$$

For improving optimization's flexibility of fuzzy controller, numerous scaling factors are applied to the outputs.

$$Outer\ loop:\ U_1^*(t) GC_1 = U_1(t) \tag{19}$$

$$Inner\ loop:\ U_2^*(t) GC_2 = U_2(t) \tag{20}$$

The output variable of controller, which indicate variations in control, is made up of the following membership functions: $NM\left(m_2\right), NB\left(m_3\right), PM\left(m_2\right), PB\left(m_3\right), NS\left(m_1\right), PS\left(m_1\right)$ and $ZO\left(0\right)$. The primary variables of the membership functions are identical to m_1, m_2 and m_3. Fig. 7 displays the use of triangle membership functions for fuzzy sets developed in an input space. With their modifications, the fuzzy cascade controller has now reached its ideal state. By changing the position, the fuzzy controller adjusts the lever arm's angle to the proper value. Regulating an outside portion is difficult, nevertheless, when the inner loop's

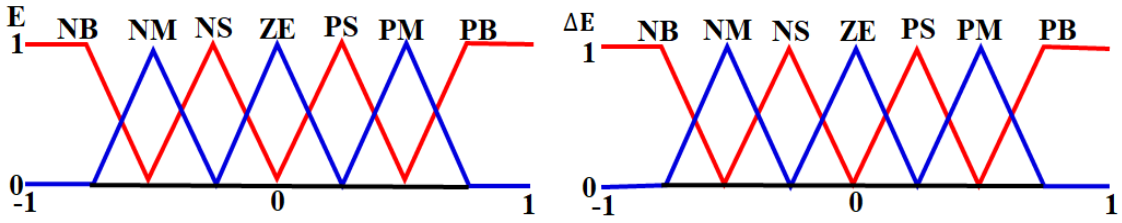

Fig. 7. Membership functions.

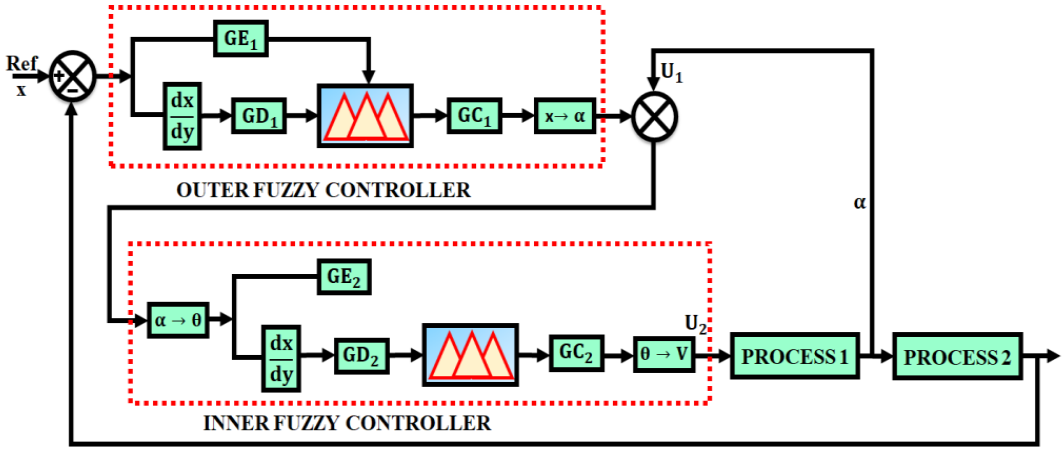

Fig. 8. Structure of Cascaded fuzzy controller.

output fluctuates a lot. It optimizes the variables of the fuzzy cascaded controller to get higher dynamic characteristics of the systems under control. As a consequence, an improved performance has been attained by the altered membership functions. Nevertheless, regulating an outside portion is difficult when the inner loop's output fluctuates a lot. By optimizing the variables of the fuzzy cascade controller, the dynamic properties of the systems under control are improved. Consequently, the altered membership functions have achieved improved performance. Then, the converter's output is converted into an AC voltage, and isolation is offered by an isolation transformer to alleviate harmonic distortion on the load and source side. For transforming the AC into a DC supply, the interleaved synchronous rectifier is exploited, and PI controller is used to manage it.

2- 4- Interleaved Synchronous Rectifier

An interleaved synchronous rectifier is a device that transforms AC into DC power are frequently found in load applications and battery chargers. It makes use of synchronous rectification, a method that increases efficiency by substituting actively controlled switches, such as power MOSFETs, for diodes. For efficient power supply, the rectified DC supply is delivered to the low-voltage DC bus.

3- Results and Discussion

The research is applied in MATLAB, and the results of the PV-based Cascaded fuzzy MPPT controller is analyzed. The comparison between developed and conventional approaches is included in this part. Table 2 depicts the parameter specification of this research.

The characteristics of the PV system are displayed in Fig. 9. The temperature is sustained at $30^{o}C$ while the intensity is settled at $1000(W/Sq.m)$ in the complete system. Then, the voltage on the input side is maintained at 100 V, and the current on the input side is settled at 25 A throughout the system.

Fig. 10 represents the ISZ converter output's waveform, and its voltage is quickly increased and continued at 390 V while its current is also gradually elevated and sustained at 5.5 A with no oscillations.

The waveforms of power are depicted in Fig. 11. The input power is randomly altered and stabilized at 2500 V, and the output power is raised and continued at 2200 W with no

Table 2. Parameters of developed research.

Parameter	Specification
PV System	
Voltage (Open Circuit)	37.25V
Panels in Parallel	32
Cell in Series	36
Current (Short Circuit)	8.95A
Panels in series	2
Rated Power	10kW
IMPROVED SEPIC-ZETA CONVERTER	
L_1, L_2, L_3	1 mH
Switching frequency	10KHz
C_1, C_2, C_3	22µF
C_0	2200 µF

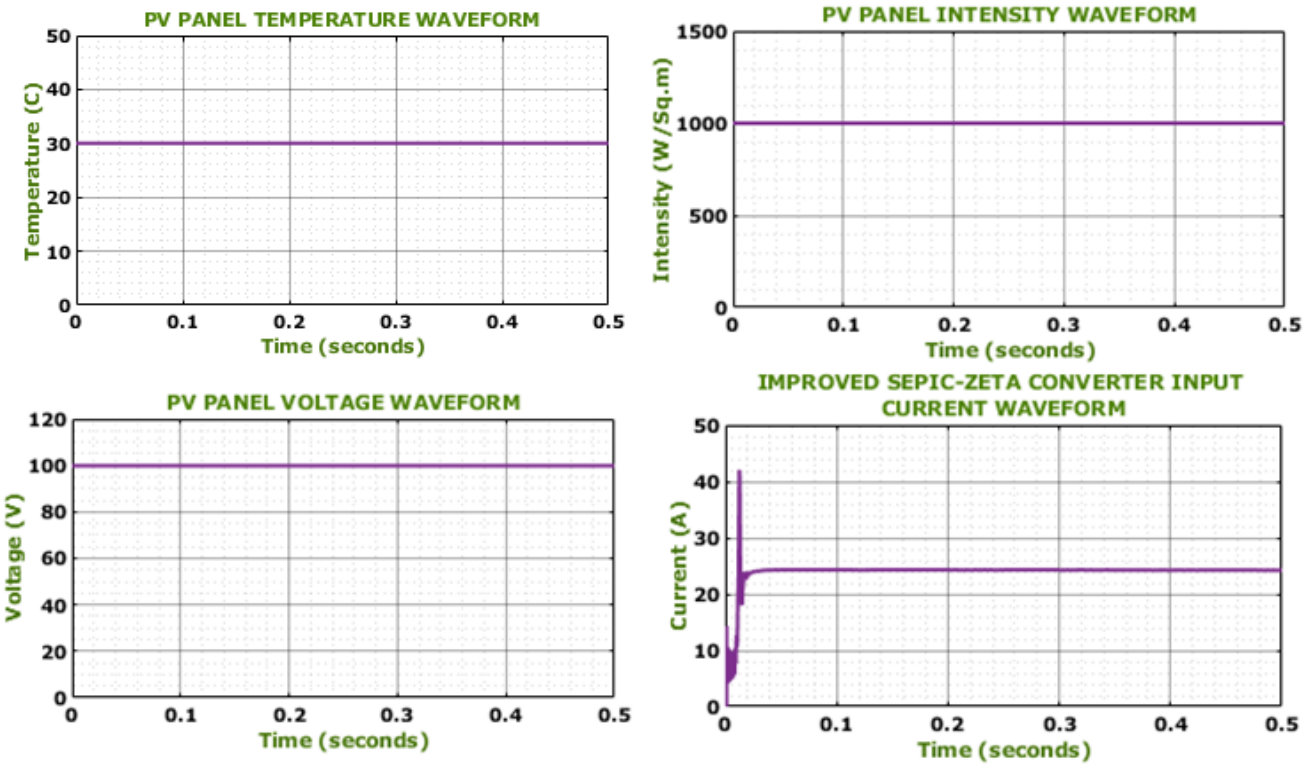

Fig. 9. Characteristics of PV system.

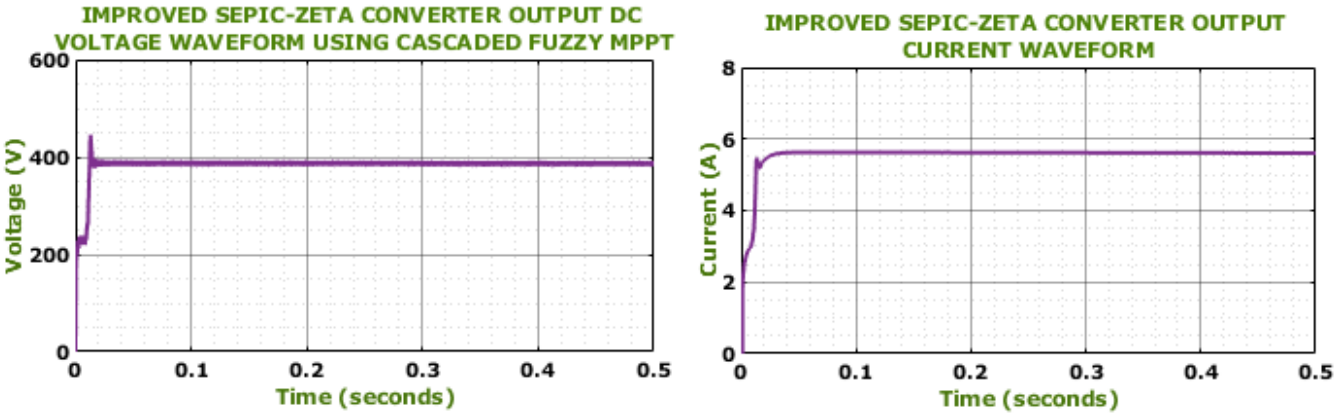

Fig. 10. ISZ Converter output.

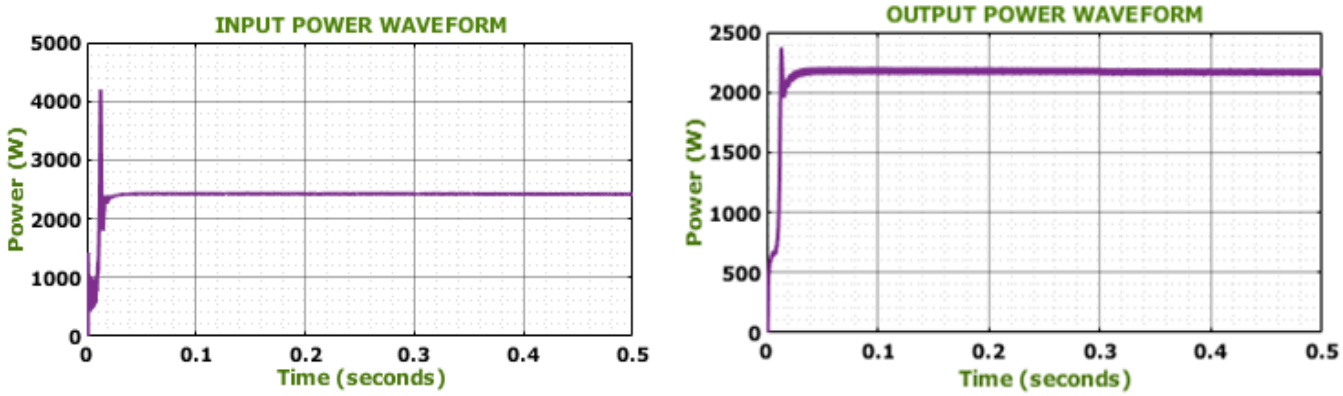

Fig. 11. Waveforms of power

oscillations.

Fig. 12 reveals the waveforms of voltage for the rectifier and HFI. Here, the rectifier's voltage on the output side is maintained at 220 V while the inverter and transformer are set at 320 V and 100 V in the entire system.

The output waveforms of the synchronous rectifier are revealed in Fig. 13. The voltage of the rectifiers 1 and 2 on the output side is settled at 105 V, while the rectifier 1 and 2's current on the output side is settled at 3.2 A in the entire system.

The behaviour of the PV system is presented in Fig. 14. The temperature is altered in the starting period and maintained at 35 ^{o}C. The intensity waveform denotes that the solar intensity received by the solar panel, which is initially varied and steadied at $1000(W/Sq.m)$. The voltage is changed in the early stage and finally continues at $100V$. The current is arbitrarily varied in the initial period and continued at $25A$ without any oscillations.

Fig. 15 represents the output waveforms of the ISZ converter. There is an arbitrary deviation in the output voltage, which is stabilized at $410V$ with the help of a cascaded fuzzy MPPT algorithm. Then, the output current is arbitrarily varied in the initial period and continued at $5.8A$ without any oscillations.

The waveforms of power are shown in Fig. 16. Initially, there is an arbitrary variation in input power, and it is stabilized at $2500W$ with no distortions. The output power is varied arbitrarily in the early stage and sustained to $2250W$ with distortions.

Fig. 17 depicts the waveforms of voltage. The output voltage of the synchronous rectifier is gradually enhanced in

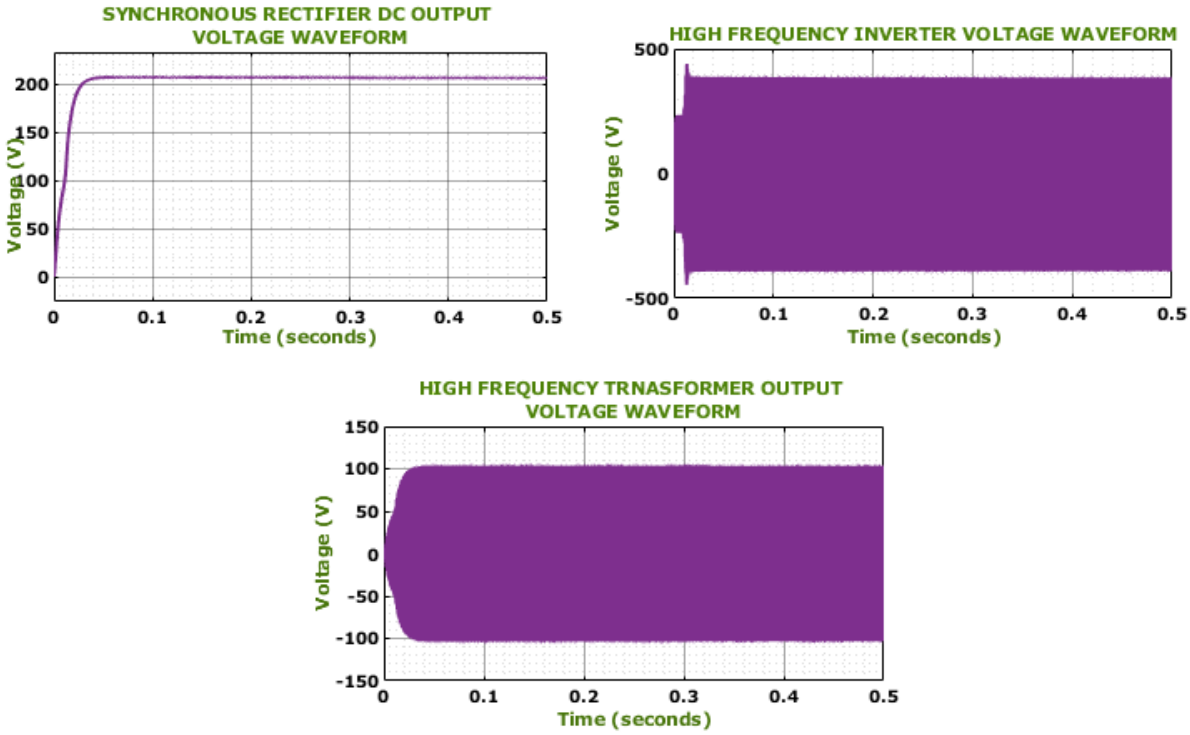

Fig. 12. Waveforms of voltage for rectifier and HFI.

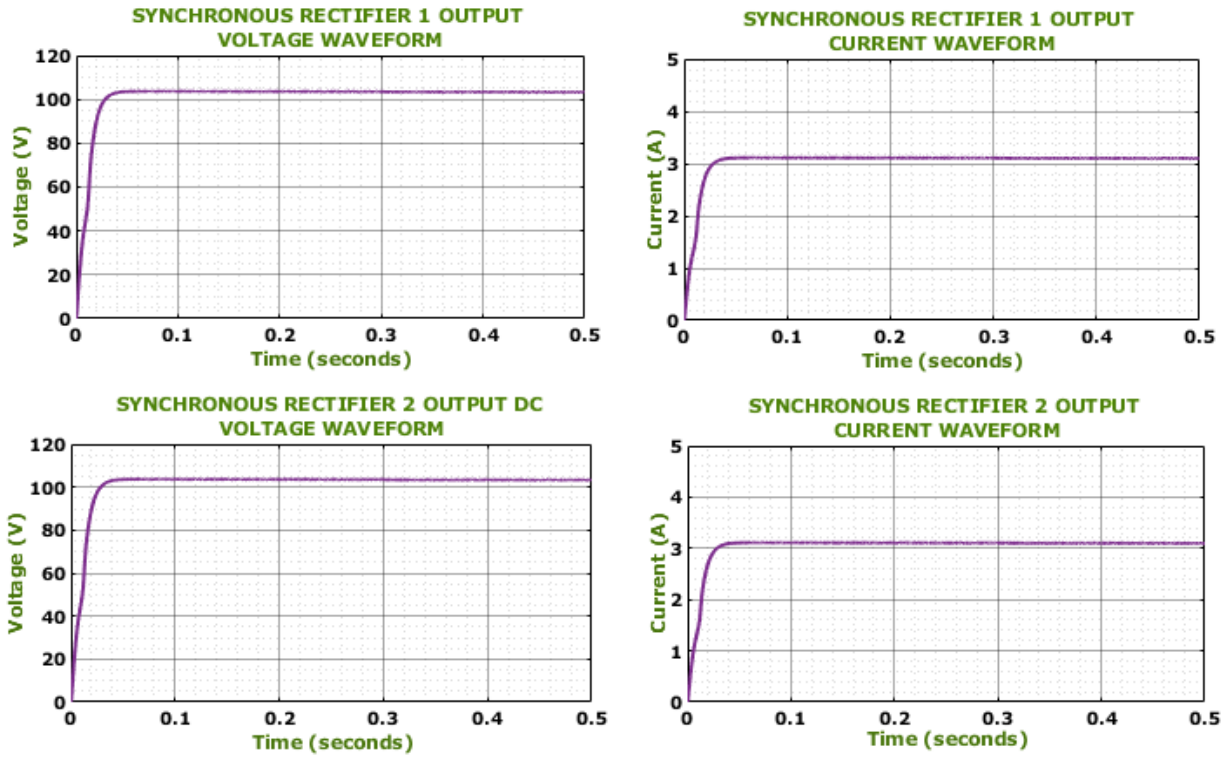

Fig. 13. Output waveforms of synchronous rectifier.

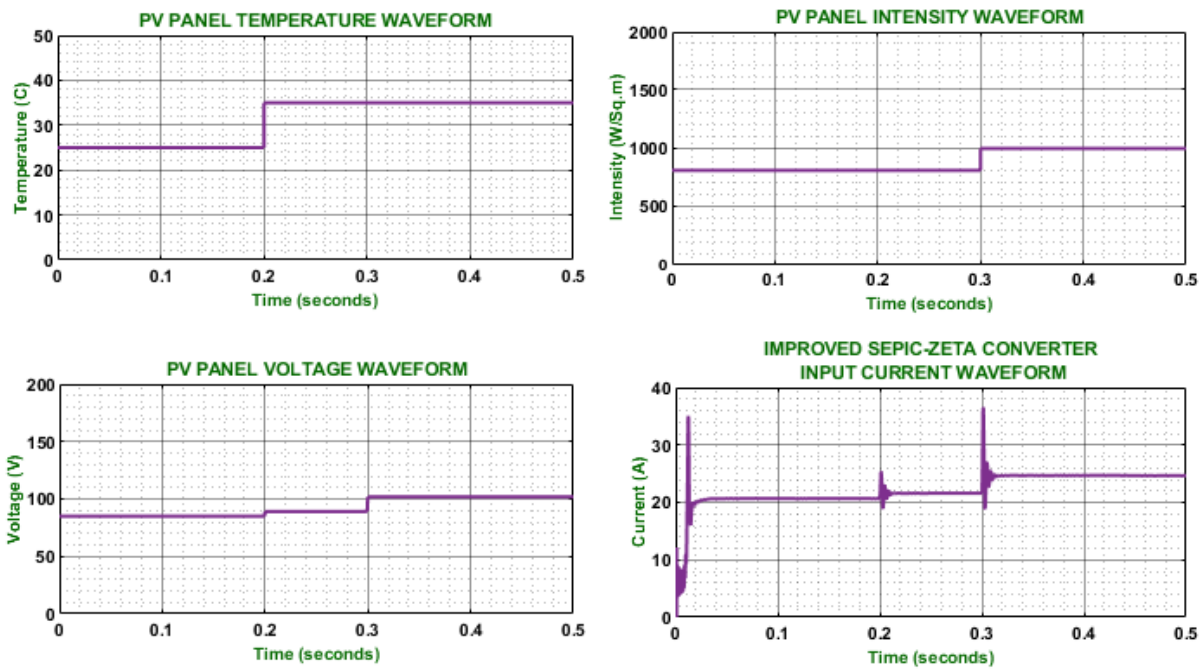

Fig. 14. Waveforms of PV system.

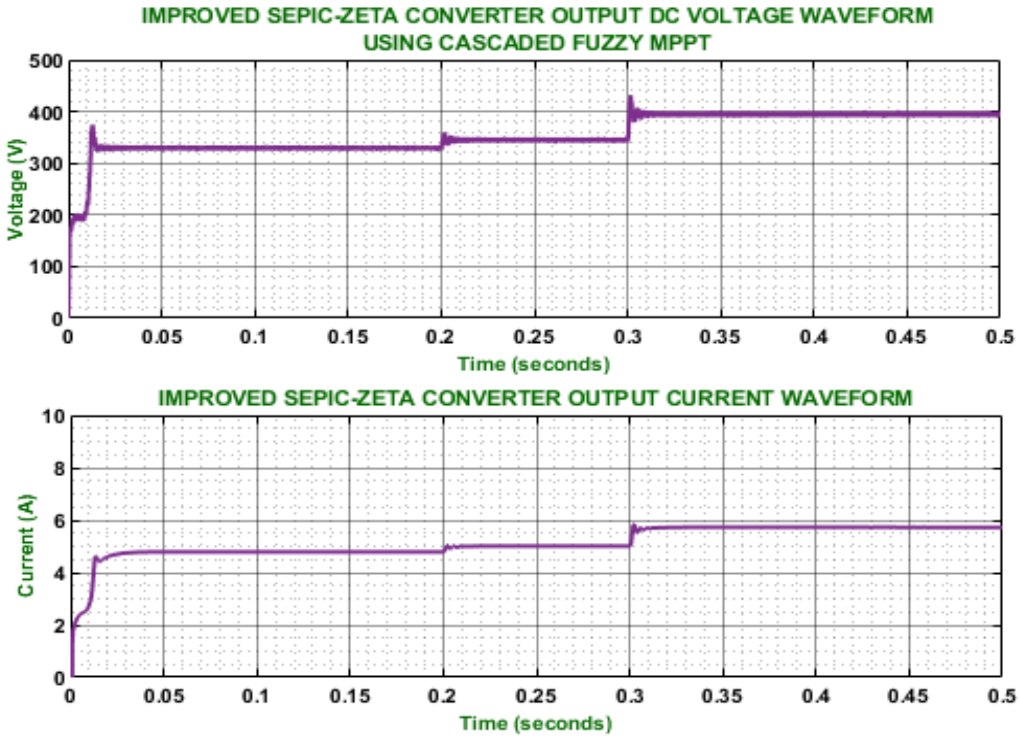

Fig. 15. ISZ converter output.

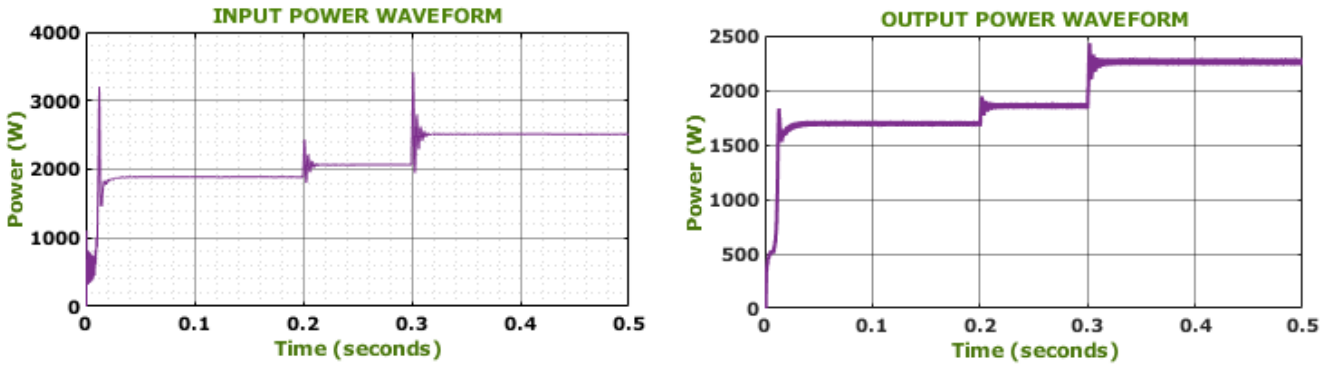

Fig. 16. Waveforms of power.

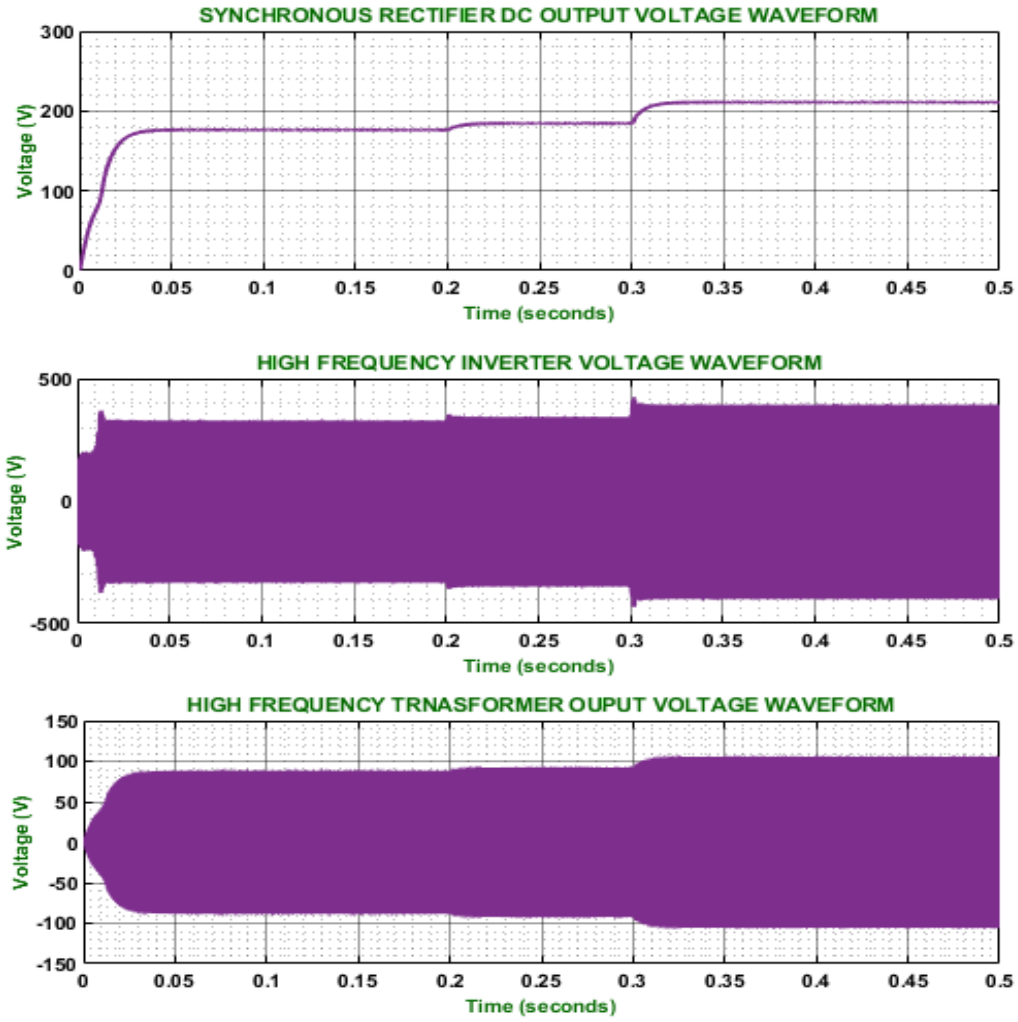

Fig. 17. Waveforms of voltage for rectifier and HFI.

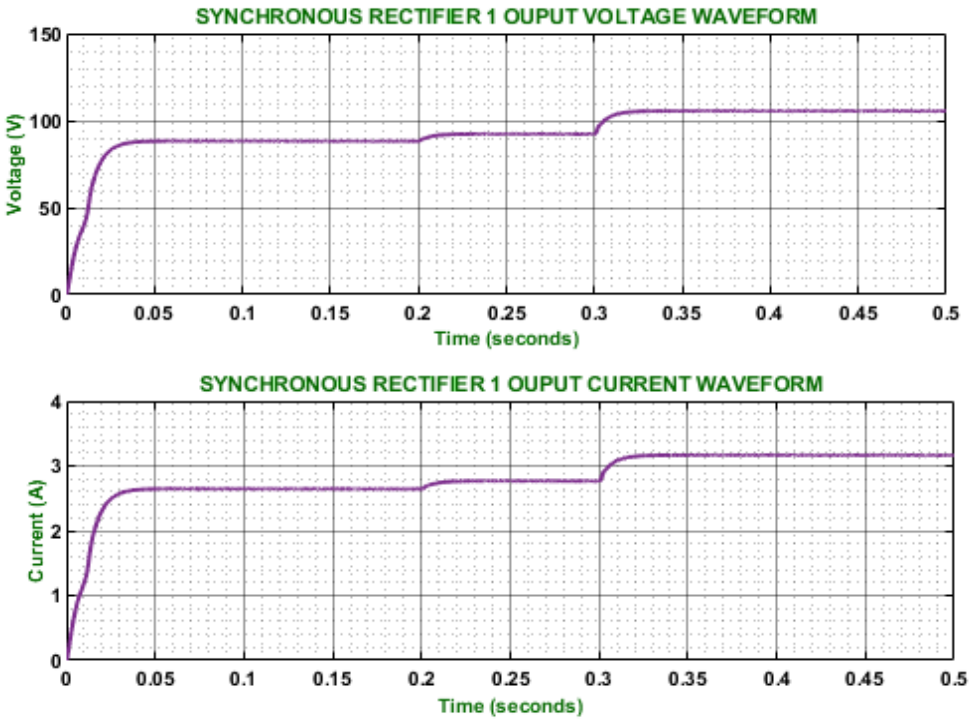

Fig. 18. Output waveforms of synchronous rectifier 1.

the early time and steadied at $220V$ with slight fluctuations. The voltage HFI is varied slowly in the starting period and stabilized at $400V$. Consequently, the output voltage of the high-frequency transformer is varied in the beginning and continues to $110V$.

An output waveform of synchronous rectifier 1 is depicted in Fig. 18. The output voltage is progressively raised in the initial period and maintained at $110V$ with no distortions. The output current is changed at the start and sustained to $3.2A$ without any fluctuations. Fig. 19 indicates the output waveforms of synchronous rectifier 2. There is an arbitrary variation in the initial time of the output voltage, and is continued at $110V$. Subsequently, the output current is changed in the beginning and is sustained at $3.2A$ with little distortions.

The waveform of the PV system in the partial shading condition is depicted in Fig. 20. Here, the temperature is initially raised and settles at $25^{o}C$ while the intensity is maintained at $950(W/Sq.m)$ and its current on the input side is arbitrarily altered in the early stage and stabilized at 23 A, and its voltage on the input side is settled at 95 A with no oscillations.

Fig 21 depicts the ISZ converter's output responses, and its voltage is progressively elevated and sustained at 375 V while its current is suddenly decreased and sustained at 5.7 A without fluctuations in the entire system.

The responses of power are represented in Fig 22. An input power is subjectively altered in the initial stage and continued at 2200 V, while the output power is settled at 1900 V in the entire system.

The analysis of efficiency between interleaved boost [30], KY [31], and ISZ converter is represented in Table 3. Compared to the interleaved boost and KY converter, the ISZ converter has a maximum efficacy of 95.12 %, which improves the energy conversion efficacy.

Fig. 23 represents the graph of the voltage gain versus duty cycle. The converters, such as transformerless high gain boost [32], non-inverting [33], and high step-up [34] converter achieves the lowest voltage gain than the ISZ converter.

The analysis of switch stress with voltage gain is illustrated in Fig. 24. The ISZ converter has the lowest stress than transformer less high gain boost [32], non-inverting DC/DC [33], and high step-up [34] converters.

Table 4 displays the performance analysis of Ant Colony Optimization (ACO) [35], Modified Deterministic JAYA [36] and proposed MPPT approach. The lowest tracking efficiency is attained by ACO (99.75%), Modified Deterministic JAYA (99.22 %) compared to developed MPPT approach (99.77%).

An analysis of existing with ISZ converter is depicted in Table 5. Here, the proposed converter has the least count of components than Switched inductor/capacitor [37], Interleaved [38], High step-up [39] and ISZ converter.

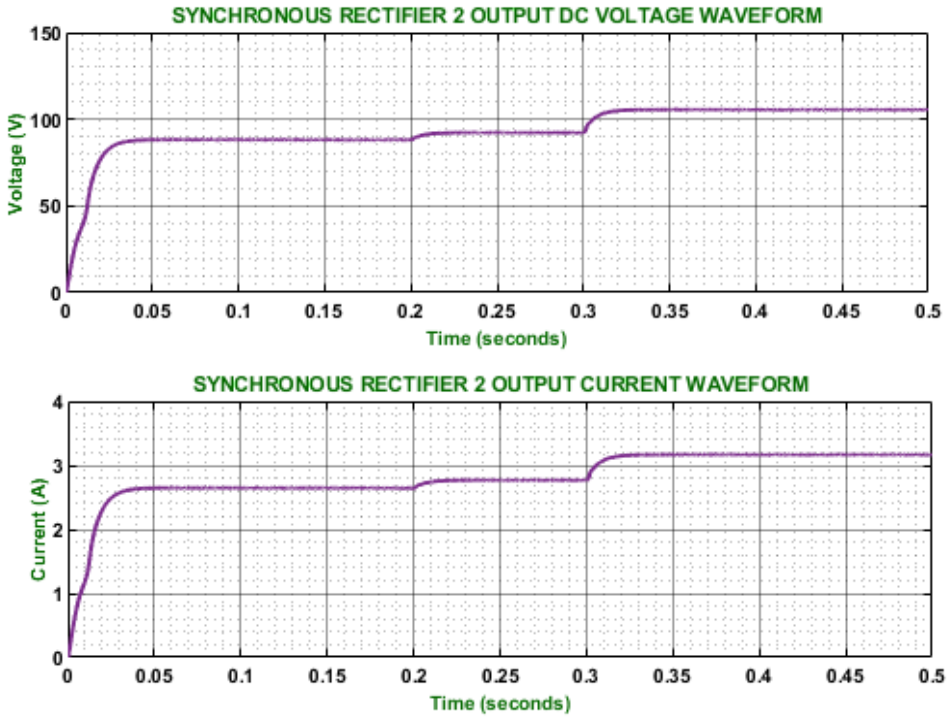

Fig. 19. Responses of synchronous rectifier 2.

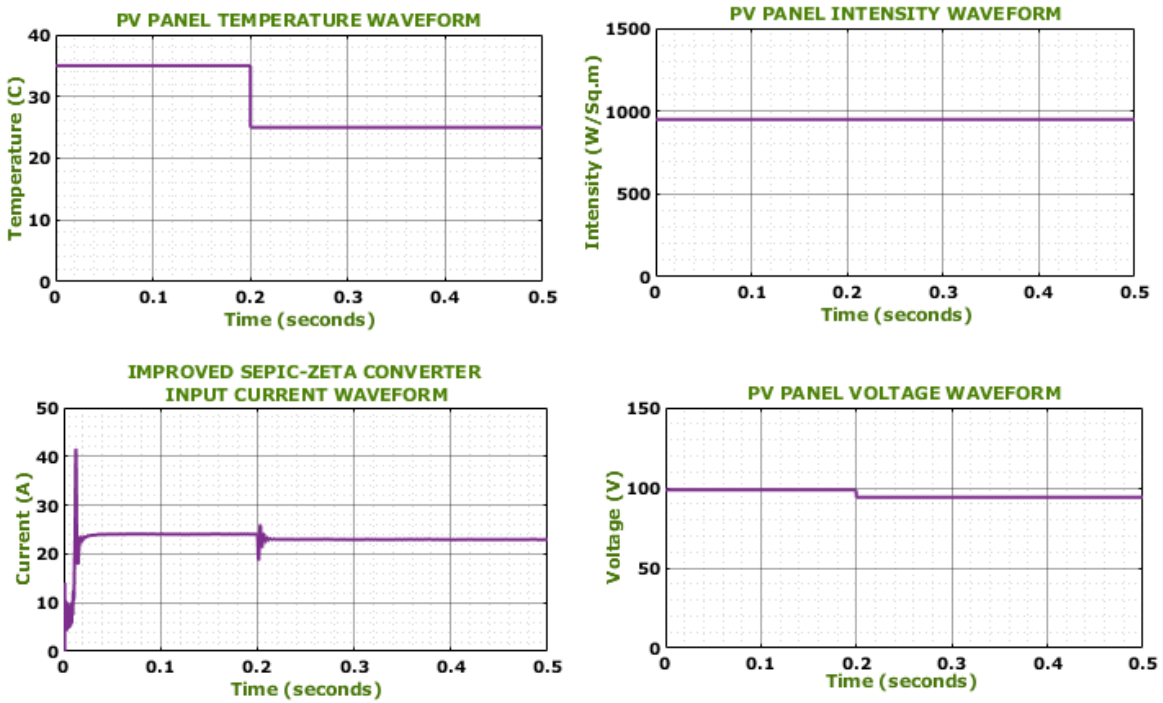

Fig. 20. Waveform of PV system.

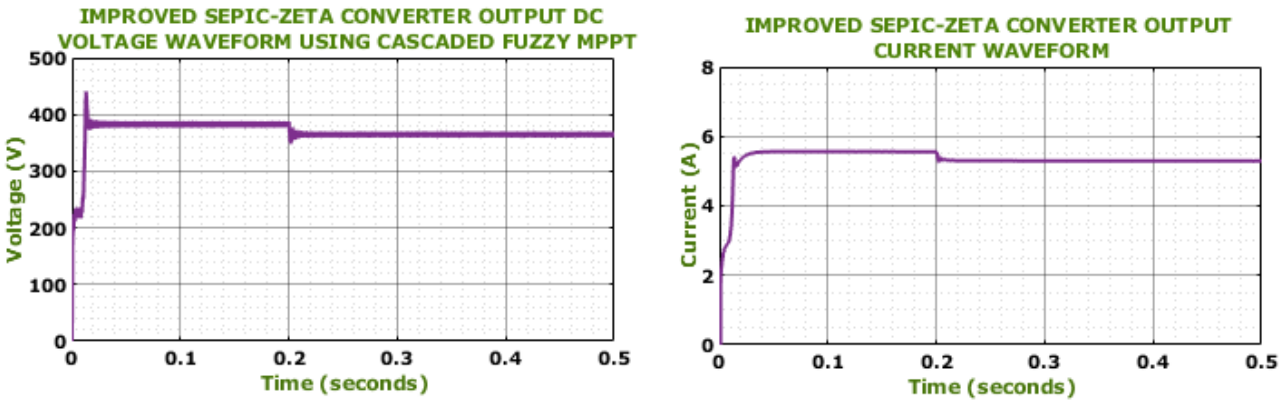

Fig. 21. Output waveform of the ISZ converter.

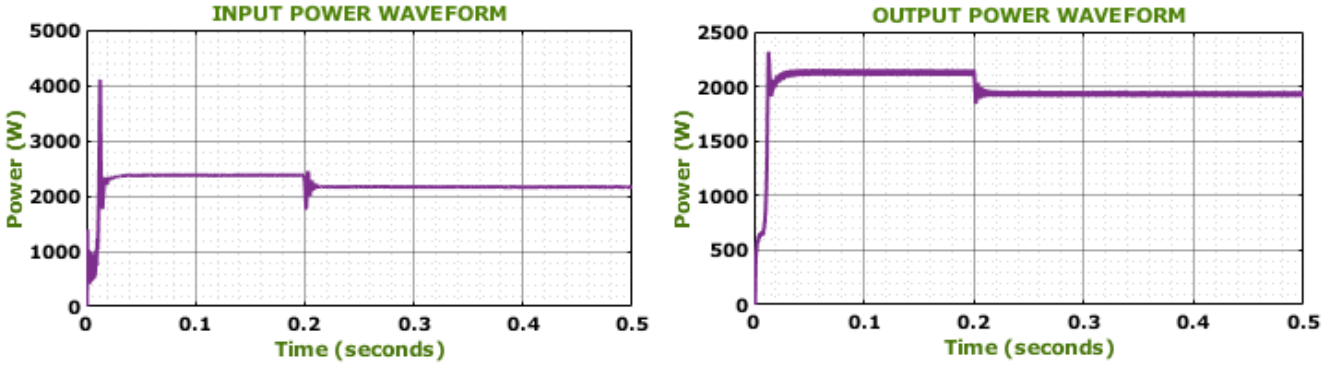

Fig. 22. Power responses.

Table 3. Comparison of efficiency.

Converters	Efficiency in %
Interleaved boost	93
KY	93
Proposed	95.12

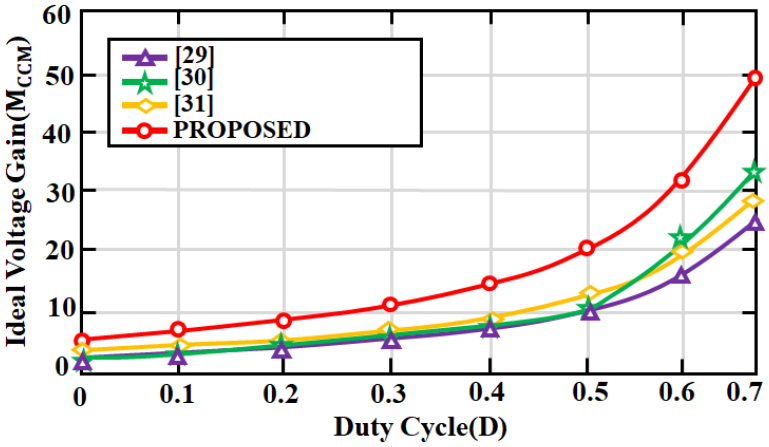

Fig. 23. Analysis of voltage gain.

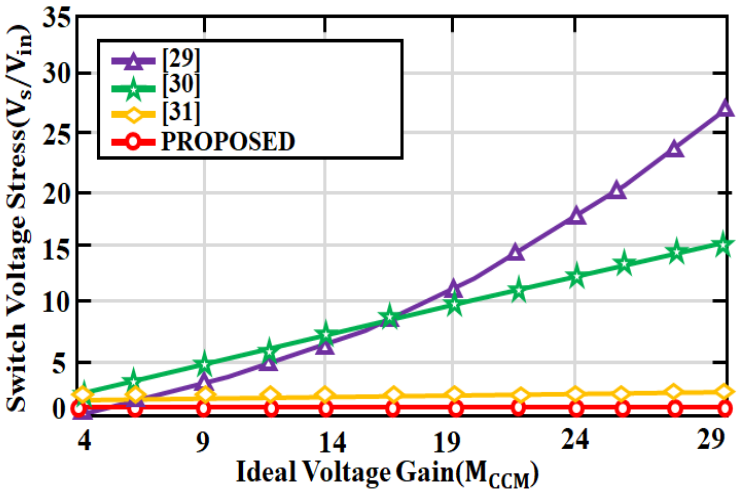

Fig. 24. Analysis of switch stress with voltage gain

Table 4. Analysis of tracking efficiency.

MPPT approaches	Tracking efficiency in %
ACO	99.75
DM JAYA	99.22
Proposed	99.77

Table 5. Analysis of existing converters.

Converters	Voltage gain	Component count
Switched inductor/capacitor converter [37]	$\frac{1+3D_1-D_2}{1-D_1-D_2}$	16
Interleaved converter [38]	$\frac{2(1+D_1)}{1-D_1-D_2}$	12
High step-up converter [39]	$\frac{4D_1+2D_2}{1-D_1-D_2}$	14
Proposed converter	$\frac{1}{1-D}$	7

4- Conclusion

This research presents the ISZ converter with a Cascaded fuzzy MPPT algorithm for efficient power transfer. The ISZ converter enhances the efficacy and performance of the overall system. Cascaded fuzzy MPPT algorithm optimizes the output power by regulating the operating points of the PV panels. Subsequently, the high-frequency inverter and isolation transformer enhance the reliability of the power transfer system by delivering stable power. Current ripple and losses are effectively minimized by an interleaved synchronous rectifier, leading to higher efficacy in power conversion that increases the reliability of the system. The overall work is validated in MATLAB, proving the developed work has the converter efficacy of 95.12 % with the highest voltage gain, endorsing the system's efficacy and reliability in power transfer.

References

[1] M. H. Zafar, N. M. Khan, M. Mansoor, A. F. Mirza, S. K. R. Moosavi, and F. Sanfilippo, "Adaptive ML-based technique for renewable energy system power forecasting in hybrid PV-Wind farms power conversion systems," 2022 Energy Conversion and Management, vol. 258, pp. 115564, doi: https://doi.org/10.1016/j.enconman.2022.115564.

[2] M. S. Javed, T. Ma, J. Jurasz, F. A. Canales, S. Lin, S. Ahmed, and Y. Zhang, "Economic analysis and optimization of a renewable energy-based power supply system with different energy storage for a remote island," 2021 Renewable Energy, vol. 164, pp.1376-1394, doi: https://doi.org/10.1016/j.renene.2020.10.063.

[3] G. M. Jagadeesan, R. Pitchaimuthu, and M. Sridharan, "A two-stage single-phase grid-connected solar-PV system with simplified power regulation," 2022 Chinese Journal of Electrical Engineering, vol. 8, no. 1, pp. 81-92, doi: https://doi.org/10.23919/CJEE.2022.000008.

[4] Z. Zakria, S. I. Khan, E. Khalaji, H. S. Munawar, F. Al-Turjman, M. A. P. Mahmud, A. Z. Kouzani, and K. Le, "Predicting the energy output of hybrid PV–wind renewable energy system using feature selection technique for smart grids," 2021 Energy Reports, vol. 7, pp. 8465-8475, doi: https://doi.org/10.1016/j.egyr.2021.01.018.

[5] E. M. Molla and C. C. Kuo, "Voltage sag enhancement of grid connected hybrid PV-wind power system using battery and SMES-based dynamic voltage restorer," 2020 IEEE Access, vol. 8, pp. 130003-130013, doi: https://doi.org/10.1109/ACCESS.2020.3009420.

[6] V. B. M. Krishna, V. Sandeep, B. K. Narendra, and K. R. K. V. Prasad, "Experimental study on self-excited induction generator for small-scale isolated rural electricity applications," 2023 Results in Engineering, vol. 18, pp. 101182, doi: https://doi.org/10.1016/j.rineng.2023.101182.

[7] A. K. Behura, A. Kumar, D. K. Rajak, C. I. Pruncu, and L. Lamberti, "Towards better performances for a novel rooftop solar PV system," 2021 Solar Energy, vol. 216, pp. 518-529, doi: https://doi.org/10.1016/j.solener.2021.01.045.

[8] N. F. Ibrahim, M. M. Mahmoud, A. M. H. Al Thaiban, A. B. Barnawi, Z. M. S. Elbarbary, A. I. Omar, and H. Abdelfattah, "Operation of grid-connected PV system with ANN-based MPPT and an optimized LCL filter using GRG algorithm for enhanced power quality," 2023 IEEE Access, doi: https://doi.org/10.1109/ACCESS.2023.3317980.

[9] L. Al-Ghussain, R. Samu, O. Taylan, and M. Fahrioglu, "Sizing renewable energy systems with energy storage systems in microgrids for maximum cost-efficient utilization of renewable energy resources," 2020 Sustainable Cities and Society, vol. 55, pp. 102059, doi:

https://doi.org/10.1016/j.scs.2020.102059.

[10] S. Obukhov, A. Ibrahim, A. A. Z. Diab, A. S. Al-Sumaiti, and R. Aboelsaud, "Optimal performance of dynamic particle swarm optimization-based maximum power trackers for stand-alone PV systems under partial shading conditions," 2020 IEEE Access, vol. 8, pp. 20770-20785, doi: https://doi.org/10.1109/ACCESS.2020.2966430.

[11] M. Takruri, M. Farhat, O. Barambones, J. A. Ramos-Hernanz, M. J. Turkieh, M. Badawi, H. AlZoubi, and M. Abdus Sakur, "Maximum power point tracking of PV system based on machine learning," 2020 Energies,vol. 13, no. 3,pp. 692, doi: https://doi.org/10.3390/en13030692.

[12] S. Sharma, L. Varshney, R. M. Elavarasan, A. S. S. Vardhan, A. S. S. Vardhan, R. K. Saket, U. Subramaniam, and E. Hossain, "Performance enhancement of PV system configurations under partial shading conditions using MS method," 2021 IEEE Access, vol. 9, pp. 56630-56644, doi: https://doi.org/10.1109/ACCESS.2021.3071340.

[13] P. Puranen, A. Kosonen, and J. Ahola, "Technical feasibility evaluation of a solar PV-based off-grid domestic energy system with battery and hydrogen energy storage in northern climates," 2021 Solar Energy, vol. 213, pp. 246-259, doi: https://doi.org/10.1016/j.solener.2020.10.089.

[14] K. S. Kavin, P. Subha Karuvelam, M. Devesh Raj, and M. Sivasubramanian, "A Novel KSK Converter with Machine Learning MPPT for PV Applications," 2024 Electric Power Components and Systems, pp. 1-19, doi: https://doi.org/10.1080/15325008.2024.2346806.

[15] O. Andrés-Martínez, A. Flores-Tlacuahuac, O. F. Ruiz-Martinez, and J. C. Mayo-Maldonado, "Nonlinear model predictive stabilization of DC–DC boost converters with constant power loads," 2020 IEEE Journal of Emerging and Selected Topics in Power Electronics, vol. 9, no. 1, pp. 822-830, doi: https://doi.org/10.1109/JESTPE.2020.2964674.

[16] H. C. Mohanta, B. T. Geetha, M. S. Alzaidi, I. S. Dhanoa, P. Bhambri, U. Mamodiya, and R. Akwafo, "An Optimized PI Controller-Based SEPIC Converter for Microgrid-Interactive Hybrid Renewable Power Sources," 2022 Wireless Communications and Mobile Computing, no. 1, pp.6574825, doi: https://doi.org/10.1155/2022/6574825.

[17] E. Şehirli, "Analysis of LCL Filter Topologies for DC-DC Isolated Cuk Converter at CCM Operation", 2022 in IEEE Access, vol. 10, pp. 113741-113755, doi: https://doi.org/10.1109/ACCESS.2022.3218162.

[18] B. Zhu, G. Liu, Y. Zhang, Y. Huang, and S.Hu, "Single-switch high step-up zeta converter based on coat circuit," 2020 IEEE Access, vol. 9, pp.5166-5176, doi: https://doi.org/10.1109/ACCESS.2020.3048388.

[19] O. Abdel-Rahim, M. L. Alghaythi, M. S. Alshammari, and D. S. M. Osheba, "Enhancing Photovoltaic Conversion Efficiency With Model Predictive Control-Based Sensor-Reduced Maximum Power Point Tracking in Modified SEPIC Converters," 2023 in IEEE Access, vol. 11, pp. 100769-100780, doi: https://doi.org/10.1109/ACCESS.2023.3315150.

[20] C. Pradhan, M. K. Senapati, S. G. Malla, P. K. Nayak, and T. Gjengedal, "Coordinated power management and control of standalone PV-hybrid system with modified IWO-based MPPT," 2020 IEEE Systems Journal, vol. 15, no. 3, pp. 3585-3596, doi: https://doi.org/10.1109/JSYST.2020.3020275.

[21] O. Abdel-Rahim and H. Wang, "A new high-gain DC-DC converter with model-predictive-control based MPPT technique for photovoltaic systems," 2020 CPSS Transactions on Power Electronics and Applications, vol. 5, no. 2, pp.191-200, doi: https://doi.org/10.24295/CPSSTPEA.2020.00016.

[22] A. Harrison, E. M. Nfah, J. de Dieu Nguimfack Ndongmo, and N. H. Alombah, "An Enhanced P&O MPPT Algorithm for PV Systems with Fast Dynamic and Steady-State Response under Real Irradiance and Temperature Conditions," 2022 International Journal of Photoenergy, no. 1, 6009632, doi: https://doi.org/10.1155/2022/6009632.

[23] B. Sabir, S. D. Lu, H. D. Liu, C. H. Lin, A. Sarwar, and L. Y. Huang, "A novel isolated intelligent adjustable buck-boost converter with hill climbing MPPT algorithm for solar power systems," 2023 Processes, vol. 11, no. 4, pp.1010, doi: https://doi.org/10.3390/pr11041010.

[24] L. Shang, H. Guo, and W. Zhu, "An Improved MPPT Control Strategy Based on Incremental Conductance Algorithm," 2020 in Protection and Control of Modern Power Systems, vol. 5, no. 2, pp. 1-8, doi: https://doi.org/10.1186/s41601-020-00161-z.

[25] C. González-Castaño, C. Restrepo, S. Kouro, and J. Rodriguez, "MPPT algorithm based on artificial bee colony for PV system," 2021 IEEE Access, vol. 9, pp. 43121-43133, doi: https://doi.org/10.1109/ACCESS.2021.3066281.

[26] K. W. Nasser, S. J. Yaqoob, and Z. A. Hassoun, "Improved dynamic performance of photovoltaic panel using fuzzy logic-MPPT algorithm," 2021 Indonesian Journal of Electrical Engineering and Computer Science, vol. 21, no. 2, pp. 617-624.

[27] A. Goswami, P. K. Sadhu, "Stochastic firefly algorithm enabled fast charging of solar hybrid electric vehicles," 2021 Ain Shams Eng. J, vol. 12, no. 1, pp. 529–539, doi: https://doi.org/10.1016/j.asej.2020.08.016.

[28] N. Priyadarshi, M. S. Bhaskar, P. Sanjeevikumar, F. Azam, B. Khan, "High-power DC–DC converter with proposed HSFNA MPPT for photo voltaic based ultra-fast charging system of electric vehicles," 2022 IET Renew. Power Gener, vol. 16, no. 9, doi: https://doi.org/10.1049/rpg2.12513.

[29] S. B. Hamed, A. Abid, M. B. Hamed, L. Sbita, M. Bajaj, S. S. M. Ghoneim, H. M. Zawbaa, S. Kamel, "A robust MPPT approach based on first order sliding mode for triple-junction photovoltaic power system supplying electric vehicle," 2023, Energy Rep, vol. 9, pp. 4275–4297, doi: https://doi.org/10.1016/j.egyr.2023.02.086.

[30] N. Kumar, A. S. Siddiqui, R. Singh, "Intelligent Controller for Mitigating Power Quality Issues in Hybrid Fuzzy-Based Microgrid Applications," 2023 International Journal of Intelligent Systems and Applications in Engineering, vol.11, no. 2, pp. 719.

[31] C. Sathish, I. A. Chidambaram, and M. Manikandan, "Intelligent cascaded adaptive neuro fuzzy interface system controller fed KY converter for hybrid energy-based microgrid applications," 2023 Electrical Engineering & Electromechanics, vol. 1, pp. 63-70, doi: https://doi.org/10.20998/2074-272X.2023.1.09.

[32] M. Zaid, S. Khan, M. D. Siddique, A. Sarwar, J. Ahmad, Z. Sarwer, A. Iqbal, "A transformerless high gain DC–DC boost converter with reduced voltage stress," 2021 International Transactions on Electrical Energy System, vol. 31, no. 5, pp. 12877, doi: https://doi.org/10.1002/2050-7038.12877.

[33] A. Mahmood, M. Zaid, J. Ahmad, M.A. Khan, S. Khan, Z. Sifat, C. H. Lin, A. Sarwar, M. Tariq, B. Alamri, B, "A Non-Inverting High Gain DC–DC Converter with Continuous Input Current," 2021 IEEE Access, vol. 9, pp. 54710–54721, doi: https://doi.org/10.1109/ACCESS.2021.3070554.

[34] K. Varesi, N. Hassanpour, S. Saeidabadi, "Novel high step-up DC–DC converter with increased voltage gain per device and continuous input current suitable for DC microgrid applications," 2020 International Journal of Circuit Theory and Applications, vol. 48, no.10, pp. 1820, doi: https://doi.org/10.1002/cta.2804.

[35] H. Deboucha, I. Shams, S. L. Belaid, and S. Mekhilef, "A Fast GMPPT Scheme Based on Collaborative Swarm Algorithm for Partially Shaded Photovoltaic System," 2021 in IEEE Journal of Emerging and Selected Topics in Power Electronics, vol.9, no. 5, pp. 5571-5580, doi: https://doi.org/10.1109/JESTPE.2021.3071732.

[36] H. Deboucha, S. Mekhilef, S. L. Belaid, and A Guichi, "Modified deterministic Jaya (DM-Jaya)-based MPPT algorithm under partially shaded conditions for PV system," 2020 in IET Power Electronics, vol. 13, no. 10, pp. 4625-4632, doi: https://doi.org/10.1049/iet-pel.2020.0736.

[37] B. Faridpak, M. Bayat, M. Nasiri, R. Samanbakhsh, and M. Farrokhifar, "Improved hybrid switched inductor/switched capacitor DC–DC converters," 2021 IEEE Trans. Power Electron., vol. 36, no. 3, pp. 3053–3062, doi: https://doi.org/10.1109/TPEL.2020.3014278.

[38] F. Mumtaz, N. Z. Yahaya, S. T. Meraj, N. S. S. Singh, and G. E. M. Abro, "A novel non-isolated high-gain non-inverting interleaved DC–DC converter," 2023 Micromachines, vol. 14, no. 3, pp. 585, doi: https://doi.org/10.3390/mi14030585.

[39] V. Marzang, E. Babaei, H. Mehrjerdi, A. Iqbal, and S. Islam, "A high step-up DC–DC converter based on ASL and VMC for renewable energy applications," 2022 Energy Rep., vol. 8, pp. 12699–12711, doi: https://doi.org/10.1016/j.egyr.2022.09.080.

HOW TO CITE THIS ARTICLE

G. Satyanarayana, T. Amai Kiran, R. Kumar, K. Yohan, M. Ansari, Intelligent Photovoltaic Conversion System with Cascaded Fuzzy MPPT for Efficient DC Power Transfer, AUT J. Elec. Eng., 58(3) (2026) 553-570.

DOI: 10.22060/eej.2026.24324.5683